

Original Article

Cite this article: Midwinter D, Hadlari T, Dewing K, and Matthews WA (2023) Disruption and localization of sediment pathways by continental extension: Detrital-zircon provenance change from upper Triassic to lower Jurassic in the northern Sverdrup Basin, Nunavut. *Geological Magazine* **160**: 2057–2066. <https://doi.org/10.1017/S0016756824000050>

Received: 2 April 2022
Revised: 22 December 2023
Accepted: 14 February 2024
First published online: 2 April 2024

Keywords: geochronology; retro-arc basin; continental extension; Sverdrup Basin; Amerasia Basin

Corresponding author: Thomas Hadlari;
Email: thomas.hadlari@canada.ca

Disruption and localization of sediment pathways by continental extension: Detrital-zircon provenance change from upper Triassic to lower Jurassic in the northern Sverdrup Basin, Nunavut

Derrick Midwinter¹ , Thomas Hadlari¹ , Keith Dewing¹ and William A Matthews²

¹Geological Survey of Canada, 3303-33rd St NW, Calgary, AB T2L 2A7, Canada and ²University of Calgary, Department of Geosciences, Calgary, AB T2N 1N4, Canada

Abstract

Constraints on the tectonic setting of the upper Triassic to lower Jurassic in the Sverdrup Basin can be elucidated from detrital-zircon U-Pb ages. During the Triassic, there was a dual provenance system into sedimentary basins along the western and northern margins of Laurentia. One of the sediment sources was from an extra-basinal igneous source of Permian-Triassic zircon while the other source was recycled sediment eroded from older sedimentary basins. The Heiberg Formation/Group was deposited during a period of significant siliciclastic sedimentation into the basin from the upper Triassic to the lower Jurassic and comprises three members: Romulus, Fosheim and Remus. Previous work has interpreted that the Carboniferous-Permian-Triassic detrital zircon had stopped reaching the northern part of the Sverdrup Basin by deposition of the upper Heiberg Formation (lower Jurassic). New detrital-zircon age analyses from samples along the northern part of the basin spanning different horizons in the Heiberg Formation show that the typical extra-basinal signature, with abundant Carboniferous-Permian-Triassic ages, was no longer recorded during the initial deposition of the Fosheim Member during the latest Triassic. Previously published basin analysis from the Sverdrup Basin interprets syn-Jurassic extensional faults and so we relate the provenance change to the onset of extension. It is interpreted that the Sverdrup Basin transitioned from a basin that received sediment from a northern extra-basinal igneous source during deposition of the Romulus Member to an extensional basin by the deposition of the Fosheim Member in the latest Triassic, as the northern sediment source was interrupted by intervening extensional basins of the proto-Amerasia Basin.

1. Introduction

Detrital-zircon geochronology from siliciclastic sedimentary successions can provide important insight into tectonic setting and tectonic evolution of a sedimentary basin. Rift basins, in particular, are typically characterized by rift flank erosion and relatively local sedimentary provenance (e.g., Withjack *et al.* 2002; Cawood *et al.* 2012). The Sverdrup Basin formed initially as a Carboniferous rift basin and subsequent Jurassic-Cretaceous rifting culminated in opening of the Amerasia Basin (e.g., Embry & Beauchamp, 2008). The Triassic tectonic setting is less clear but, from previous studies, two predominant sediment sources into the Sverdrup Basin during the Triassic have been identified (e.g. Embry, 2009; Midwinter *et al.* 2016); one from the southern and eastern margins of the basin, and another derived from the northern margin.

The nature of the tectonic setting of the Sverdrup Basin during the Triassic was long considered tectonically quiescent (e.g. Embry & Beauchamp, 2008). The presence of Triassic detrital zircon within Triassic strata (Miller *et al.* 2006; Omma *et al.* 2011) led to interpretations that sedimentary provenance was from the Polar Urals (e.g., Miller *et al.* 2013; Anfinson *et al.* 2016) and that sedimentary systems that traversed the greater Barents Sea Basin (e.g., Gilmullina *et al.* 2022; Klausen *et al.* 2022) directed sediment into the Sverdrup Basin (Miller *et al.* 2013). Observations of volcanic ash beds and syn-depositional detrital-zircon ages through the late Permian to late Triassic indicate volcanism proximal to the northwestern margin of the basin (Midwinter *et al.* 2016; Hadlari *et al.* 2018; Alonso-Torres *et al.* 2018). From the combination of Permian-Triassic volcanism and syn-depositional zircon, it has been proposed that there was a magmatic arc to the north of the basin during the late Permian and Triassic, and that the Sverdrup Basin was in a retro-arc position during that time (Hadlari *et al.* 2017; Alonso-Torres *et al.* 2018; Hadlari *et al.* 2018). The detrital-zircon U-Pb age signature along the northern margin of the Sverdrup Basin is characterized by syn-depositional ages in upper Triassic strata

© The Author(s), 2024. Published by Cambridge University Press. This is an Open Access article, distributed under the terms of the Creative Commons Attribution licence (<http://creativecommons.org/licenses/by/4.0/>), which permits unrestricted re-use, distribution and reproduction, provided the original article is properly cited.



that are absent from lower and middle Jurassic strata (Omma *et al.* 2011; Midwinter *et al.* 2016), indicating the diminution of the hypothetical magmatic arc and/or the Polar Urals as a sediment source, potentially as initial rifting of the Amerasia Basin isolated the Sverdrup Basin from the extra-basinal source(s) (Embry, 2009). The Heiberg Formation/Group was deposited during this key interval with the Romulus Member in a late Triassic pre-rift setting, whereas the transition to syn-rift had taken place by deposition of the Remus member in the Early Jurassic (Pleinsbachian) (Embry, 2009; Hadlari *et al.* 2016). To accommodate uncertainties regarding the sub-Fosheim basin setting, we simply refer to the Romulus Member and older strata as 'pre-rift' (Hadlari *et al.* 2016). Deformation, uplift and erosion during the Eurekan Orogeny in the Cenozoic have obscured older faults on Axel Heiberg and Ellesmere Islands (e.g., Piepjohn & von Gosen, 2018). The best evidence for syn-rift normal faults is seismic data from Prince Patrick Island that show half-graben basins, some with the upper Heiberg Formation/Group at the base, consistent with the onset of rifting within the Heiberg Formation/Group (see discussion, Hadlari *et al.* 2016). The change in detrital-zircon provenance is determined by detrital-zircon samples from the lower (Romulus) and upper (Remus) members of the Heiberg Formation, which are grab samples collected during regional mapping (Midwinter *et al.* 2016), with no indication where this important change takes place within the intervening stratigraphy. This paper provides new detrital-zircon data from measured sections of this interval and four samples that span the boundary between the Romulus and Fosheim members (lower and middle Heiberg Formation), which serves to constrain the timing of the provenance change that is inferred to record onset of rifting in the proto-Amerasia Basin.

2. Geological setting

2.a. Sverdrup Basin

The Sverdrup Basin (Figure 1) is underlain by an up to 10 km-thick sedimentary succession of Devonian clastic wedge strata that were deformed during the Late Devonian-Early Carboniferous Ellesmerian orogeny (Embry, 1991). The Ellesmerian orogeny was succeeded by initial rifting of the Sverdrup Basin, beginning in the Carboniferous where up to 5 km of Upper Paleozoic strata accumulated in a shelf to deep-basin setting (Balkwill, 1978), and subsequently underwent significant subsidence in the Triassic followed by Early Jurassic – Early Cretaceous rifting resulting in the opening of the Amerasia Basin (e.g. Grantz *et al.* 1979, 2011; Houseknecht & Bird, 2011; Hadlari *et al.* 2016). Sediment deposited along the northern margin of the basin has been interpreted to be derived from a poorly constrained landmass that lay to the north of the basin based on sediment provenance direction (Embry, 2009). While the basin was long considered tectonically quiescent during the Triassic (e.g. Embry & Beauchamp, 2008), new data support the idea that the basin had tectonic activity, such as the observation of volcanic ash beds (Midwinter *et al.* 2016) and the undefined Triassic faults and Jurassic extensional faults at the eastern end of the Sverdrup Basin, which are parallel to the eastern flank of the Amerasia Basin (Lopez-Mir *et al.* 2018).

The Heiberg Formation in the central and eastern part of the basin is subdivided into three members, Romulus, Fosheim and Remus (Figure 2; Embry, 1983a), and is approximately 1 km thick along the eastern margin of the basin (e.g. Midwinter *et al.* 2022).

The lowermost strata in the Heiberg Formation, the Romulus Member, records a coarsening-upward succession of mudstone to fine-grained sandstone from a prodelta to delta plain environment; the overlying Fosheim Member is a coal-bearing and sandstone-rich interval deposited in a mixed alluvial-marine environment. The Romulus Member is more arkosic than the Fosheim Member, which is more quartzose. The Remus Member is a sandstone-rich unit representative of shallow marine deposits (Embry, 1983a; Midwinter *et al.* 2022). The Heiberg Formation is stratigraphically equivalent to the Heiberg Group in the western part of the basin (Embry, 1983b).

The Heiberg Group is comprised of five formations: the sandstone-rich Skybattelle Formation (equivalent to the Romulus Member), overlain by marine mudstone of the Grosvenor Island Formation, then coarsening upward into the deltaic Maclean Strait Formation, which is subsequently overlain by marine shale of the Loughheed Island Formation and ultimately capped by the sandstone-dominant King Christian Formation (Figure 2). As identified from palynological studies (Embry & Suneby, 1994), the Grosvenor Island Formation contains the Triassic-Jurassic boundary. This basin centre mudstone is correlative with thin marine mudstone in the lower portion of the Fosheim Member (Suneby & Hills, 1988; also see Hadlari *et al.* 2016). Additional evidence for this mudstone being correlative to the Grosvenor Island Formation is the presence of ironstone rubble (Midwinter *et al.* 2022), as ironstone was observed within the Grosvenor Island Formation along the southwestern margin of the Sverdrup Basin, indicative of a starved shelf (Embry & Johannessen, 1993).

The Heiberg Formation records the transition of the pre-rift stage into the syn-rift stage of the Sverdrup Basin as shallow marine sandstones prograded across the basin and multiple unconformities within the formation indicate a basin-filled state with the rift onset unconformity likely within the Fosheim Member, previously estimated to be ~200–190 Ma (Hadlari *et al.* 2016) or ~170 Ma (Embry & Beauchamp, 2008). This was supported by detrital-zircon geochronology suggesting the King Christian Formation (coeval to the upper Fosheim and Remus members) had a change in sediment source relative to the lower Heiberg Group/Formation due to the onset of rifting to the north of the Sverdrup Basin (Midwinter *et al.* 2016). This period marked the initial extension of the proto-Amerasia Basin, which could have developed as a retroarc system driven by slab rollback, which in turn rifted the Arctic Alaska-Chukotka Microplate (AACM) from northern Laurentia, thus disrupting the pathway for the northern sediment source to the Sverdrup Basin. This key transition occurred within the sedimentary succession of the Heiberg Formation, which makes samples tied to stratigraphic sections measured in the Blue Mountains and at Depot Point (Midwinter *et al.* 2022) vital to better constrain the timing of the extension.

2.a. Summary of published U-Pb provenance: Sverdrup Basin

U-Pb detrital-zircon provenance data reported from Triassic to Jurassic-aged strata from the Sverdrup Basin have a sampling gap from the upper Triassic to lower Jurassic of the Heiberg Formation/Group. Previous detrital-zircon U-Pb age studies of Triassic-aged strata (e.g. Miller *et al.* 2006; Omma *et al.* 2011; Anfinson *et al.* 2016; Midwinter *et al.* 2016; Hadlari *et al.* 2018) identified two different detrital-zircon signatures: a spectrum similar to the upper portion of the Devonian clastic wedge with a characteristic signature of 700–360 Ma ages and a broad spectrum of Meso- to Paleoproterozoic ages (Anfinson *et al.* 2012a, 2012b),

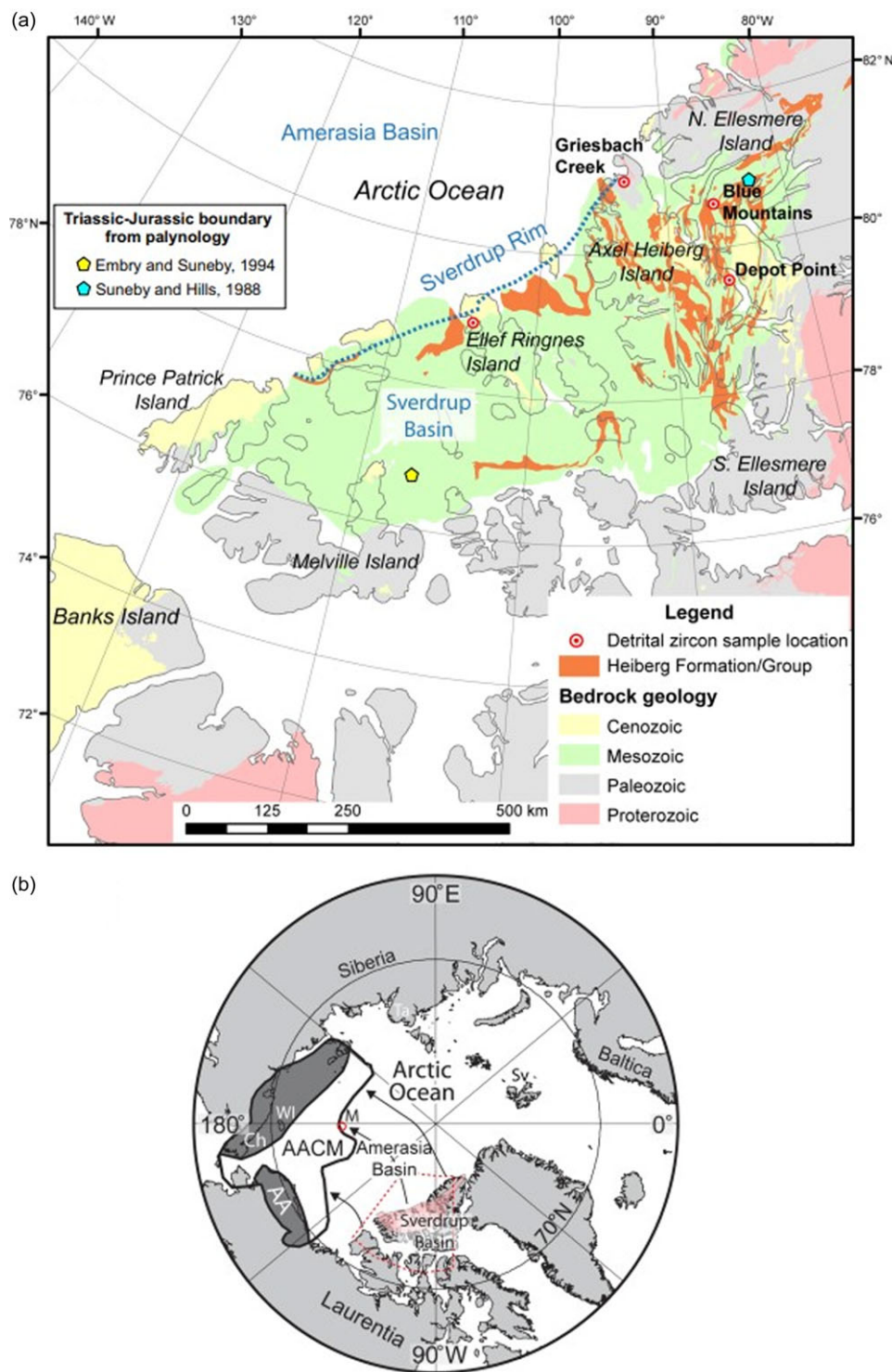


Figure 1. (Colour online) (a) Map of the Sverdrup Basin showing the location of detrital-zircon samples from the Heiberg Formation/Group. Surface and sea bottom bedrock geology is from Okulitch (1991). Detrital-zircon sample locations are from this study, Midwinter *et al.* (2016), Hadlari *et al.* (2018). See Figures 2 and 3 for stratigraphic locations of samples. (b) Map of the Arctic, depicting the basins and regions, mentioned in the text. Outline of AACM (black line) after Drachev (2011). Rotation of AACM away from the Canadian margin illustrated by black arrows (after). Red dashed line denotes location of Figure 1a. Red circle indicates the approximate location of Mendelev rise from the Shamsur Seamount sample collected by Tuchkova *et al.* (2020). AA, Arctic Alaska; AACM, Arctic Alaska - Chukotka Microplate; Ch, Chukotka; M, Mendelev rise; WI, Wrangel Island.

and Permian-Triassic grains that are near the age of deposition. Detrital-zircon samples from lower Jurassic-aged strata collected along the northern margin do not record the Carboniferous-Permian-Triassic age spectrum (Midwinter *et al.* 2016).

Previous studies used samples collected from the Heiberg Formation/Group; however, samples that are not well constrained by measured sections and/or mapping are not included in this study (e.g., Romulus Member samples from Anfinson *et al.* (2016) and the Remus Member sample from Hadlari *et al.* 2018).

Additionally, the C-numbered samples from Omma *et al.* (2011) are from the field collections of the Geological Survey of Canada (GSC), and the GSC scientist who donated them to that study asserts that the Heiberg sample is not from the upper Heiberg (Embry pers.comm., 2015), and so it is omitted. Three samples, two from the Romulus Member (measured sections) and one from the King Christian Formation (map description) (Midwinter *et al.* 2016; Hadlari *et al.* 2018), are included. In summary, previous detrital-zircon studies of the Sverdrup Basin indicate that an influx

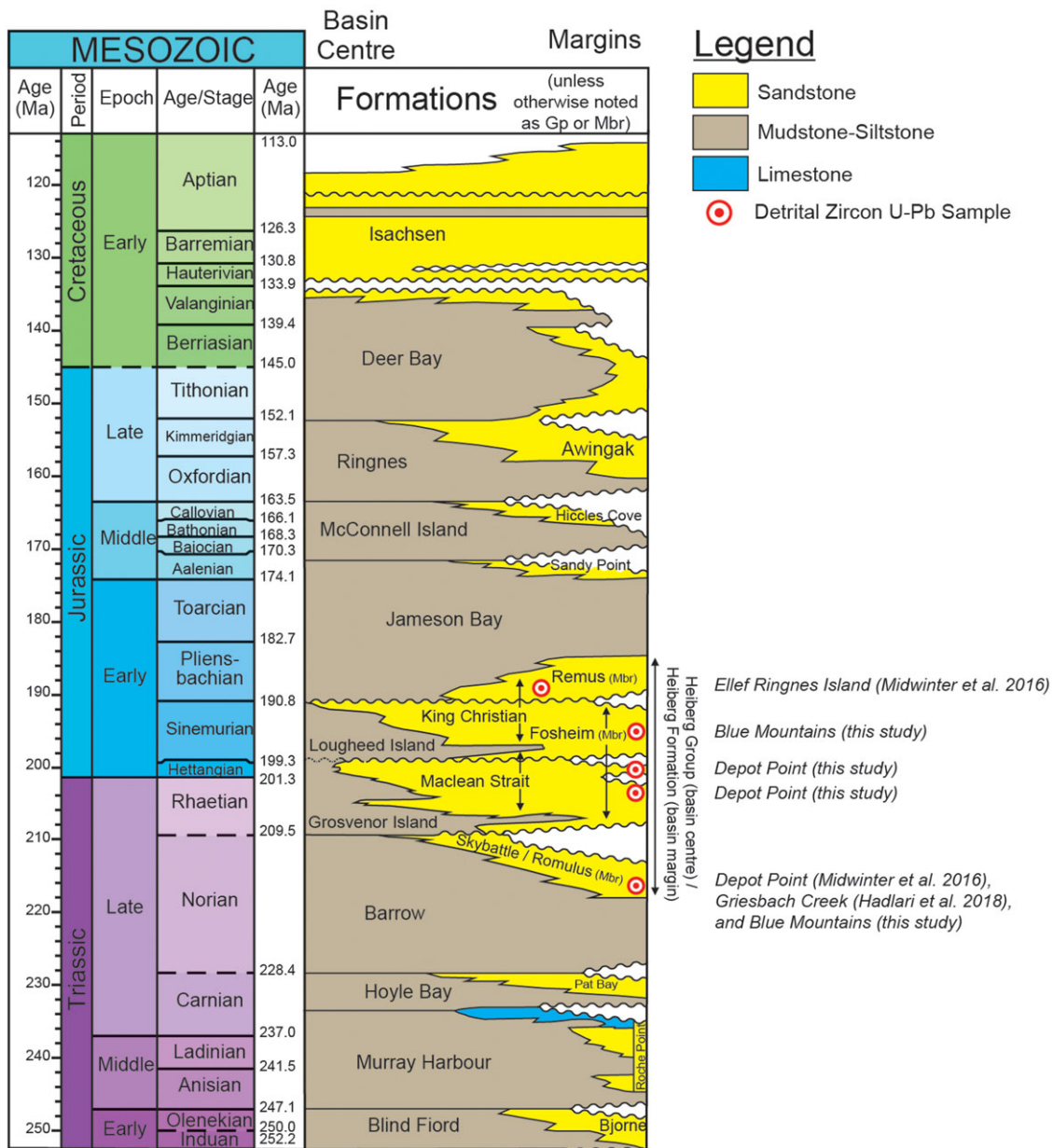


Figure 2. (Colour online) Triassic to Early Cretaceous stratigraphic chart of the Sverdrup Basin (Embry & Beauchamp, 2008; Hadlari *et al.* 2016) with location and reference of detrital-zircon samples with respect to stratigraphy.

of sediment from an igneous source to the northwest persisted through the Triassic until some point between the late Triassic and Pliensbachian.

3. Materials and methodology

A total of four new field samples are used in this study and the Supplementary Table (DR2) lists the sources of published data. Two samples were collected in 2015 from a measured section at Depot Point that spans from the upper Triassic Barrow Formation to unsubdivided Jurassic strata over an interval of 1,140 m. The Depot Point section is 40 km west of the type section for the Heiberg Formation at Buchanan Lake (Souther, 1963). One sample from the lower Romulus Member, near the contact with the Barrow Formation, was collected from a field visit to the same

location at Depot Point in 2011 with detrital-zircon geochronology results previously published (Midwinter *et al.* 2016). Two samples were collected from a measured section at the Blue Mountains on northern Ellesmere Island in 2015. The stratigraphic section started in the upper Triassic Barrow Formation and ended in the lower Jurassic Jameson Bay Formation over approximately 1,200 m. For more details on the sedimentology and stratigraphy of these measured sections, see Midwinter *et al.* (2022).

Detrital zircon was separated using standard separation techniques and isotopic signal intensities were measured for 300 grains per sample by quadrupole LA-ICP-MS (Matthews & Guest, 2017). Measurements were filtered using the calculated probability of concordance. Measurements with <1% probability of concordance were filtered from the dataset (812 of 1510 total). Dates used in the figures are ²⁰⁶Pb/²³⁸U for dates <1500 Ma and ²⁰⁷Pb/²⁰⁶Pb

for older dates. Devonian clastic wedge reference spectra are derived from Anfinson *et al.* (2012a, 2012b). Maximum depositional ages (MDA) were calculated using the YGC2 σ method (Dickinson & Gehrels, 2009), which is the weighted mean of the youngest cluster of three or more dates that overlap at 2 σ uncertainty. This approach has been shown to produce a conservative age estimate (Coutts *et al.* 2019).

4. Detrital-zircon geochronology results

Isotopic measurements yielded 812 dates that passed our filtering criteria for use in this study. Results are presented as normalized probability density and cumulative probability plots in Figure 3. Details of the isotopic results and the MDA calculations are presented in the online Supplementary Material at <http://journals.cambridge.org/geo>.

Sample *Lower Romulus – Blue Mtns* (SHF3) was collected from the lowermost sandstone of the Romulus Member (97 m, Figure 3) in the Blue Mountains, 1–2 m above the contact with the mudstone-rich Barrow Formation. The sandstone bed is fine-grained and trough and planar cross-bedded. The proportions of age groupings from $n = 184$ measurements were Archean (5%), Paleoproterozoic (18%), Mesoproterozoic (13%), 700–360 Ma (29%), Carboniferous (14%), Permian (9%) and Triassic (6%) with a near-continuous distribution of dates between 610 Ma and 209 Ma. A geologically important age fraction from 350 Ma to 200 Ma consists of 51 of 184 measurements (28%). The calculated MDA incorporates the five youngest grains and yielded a weighted mean age of 215.2 Ma \pm 9.4 (2 σ).

Sample *Lower Fosheim – Depot Pt.* (15-DTA-32-580m) was collected from a fine-grained sandstone bed immediately above the contact with the Romulus Member (580 m, Figure 3). The quartzose sandstone bed with erosional base was above the bioturbated sandstone of the Romulus Member and below a thin coal bed (Figure 3; Midwinter *et al.* 2022). The majority of the $n = 172$ measurements were Mesoproterozoic (1600–1000 Ma; 41%) and Paleoproterozoic (2500–1600 Ma; 32%). Lesser fractions were Archean (>2500 Ma; 8%) and 700–360 Ma (13%). The vast majority of measurements filtered out by probability of concordance are Proterozoic, with no apparent $^{206}\text{Pb}/^{238}\text{U}$ ages younger than 350 Ma (discordant or concordant, no ages younger than 350 Ma have been filtered out). The youngest date was 353.7 Ma \pm 16.5 (2 σ); therefore, there are no detrital-zircon grains in this sample dated between 350 Ma and 200 Ma.

Sample *Lower Fosheim – Depot Pt.* (15-DTA-32-660m) was collected from a medium-grained, quartzose, trough cross-bedded sandstone approximately 80 m above the contact with the Romulus Member (660 m, Figure 3). This sample yielded $n = 246$ measurements that passed the filtering criteria, and those that were filtered out are mainly Proterozoic with none younger than 350 Ma. The age spectrum is very similar to the basal lower Fosheim Member sample with the majority of the measurements yielding Mesoproterozoic (43%) and Paleoproterozoic (32%) dates. Other age groupings were Archean (8%) and 700–360 Ma (13%). The youngest date was 406.2 Ma \pm 9.7 (2 σ); therefore, there are no detrital-zircon grains in this sample dated between 350 Ma and 200 Ma.

Sample *Upper Fosheim – Blue Mtns* (SHF9) was collected from thinly interbedded very fine-grained quartzose sandstone with carbonaceous mudstone in the Blue Mountains (876 m, Figure 3). Additional structures observed in this sedimentary bed were wavy, ripple cross-laminations. This interval is approximately 150 m

below the contact to the Remus Member. From $n = 210$ measurements, 7% were Archean, 36% were Paleoproterozoic, 46% were Mesoproterozoic and 7% were between 700 Ma and 360 Ma. A single grain dated at 261.5 Ma \pm 12.2 (2 σ) was found between 350 Ma and 200 Ma, and none are Triassic.

5. Discussion

The collection of samples from the Heiberg Formation indicates a vertical stratigraphic transition between two provenance signatures (Figure 4). All detrital-zircon samples of the Romulus Member have a consistent and continuous age spectrum from the Carboniferous to Permian through the Triassic where the youngest-aged fraction is near the age of deposition. For example, the 350 Ma to 200 Ma age fraction in sample SHF3 composes 28% of the detrital zircon (51 of 184 measurements). Conversely, above the contact between the Romulus and Fosheim members, the detrital-zircon signature changes to a spectrum with almost no Carboniferous–Triassic age probability (1 of 628 measurements; no Triassic) that is similar to the Devonian clastic wedge reference spectrum from the Franklinian Basin that has a moderate amount of 700–360 Ma ages, a prominent peak at ca. 430–410 Ma and abundant Meso- and Paleoproterozoic ages (Figure 4). This change in detrital-zircon age signature corresponds to the lithological change from arkosic in the Romulus Member to quartzose sandstone in the Fosheim Member. Data presented here for the Fosheim Member are consistent with U–Pb detrital-zircon data also from the Fosheim Member presented by Pointon *et al.* (2023). Given that the Fosheim Member along the northern portion of the basin has only the older recycled detrital-zircon age spectrum, it can be interpreted that a shift in provenance likely occurs at the boundary between the Romulus and Fosheim members. Based on palynology from Ellesmere Island and interpreted by correlation of the member boundary to our sections, the Romulus Member is assigned a Norian to late Rhaetian age and the basal Fosheim Member consists of latest Rhaetian strata succeeded by the Triassic–Jurassic boundary interval (Suneby & Hills, 1988). In the southern portion of the Sverdrup Basin, the correlative Triassic–Jurassic boundary interval lies within the Grosvenor Formation (Embry & Suneby, 1994), and we speculate from regional correlations that the interval of the lower Fosheim Member from 588 to 607 m in the Depot Point section contains the Triassic–Jurassic boundary (Midwinter *et al.* 2022). This would place the change in provenance and rift onset unconformity as younger than Rhaetian fossils within the Romulus Member, older than the deposition of the Fosheim Member starting in the latest Rhaetian, and therefore late Rhaetian. Our estimation of the timing is dependent upon stratigraphic correlation from the sections with biostratigraphy to wells logs and our outcrop sections, which is a potential source of error and would benefit from additional geological age data.

These two distinct assemblages, a recycled source and a volcanic arc source, are exhibited in Triassic strata in sedimentary basins along the western and northern Laurentian margin, including the Sverdrup Basin, Arctic Alaska, Yukon–Tanana, Southern Canada (Quesnel and Western Interior Basin) and the Southwest U.S (Hadlari *et al.* 2017 and references therein). Triassic sedimentary rocks in Chukotka and Wrangel Island, part of the Arctic Alaska – Chukotka microplate, are potentially representative of the pre-rift source area and were most likely adjacent to the northwestern Canadian Arctic during this period (e.g. Gottlieb *et al.* 2014; Tuchkova *et al.* 2020). The detrital-zircon signature of these

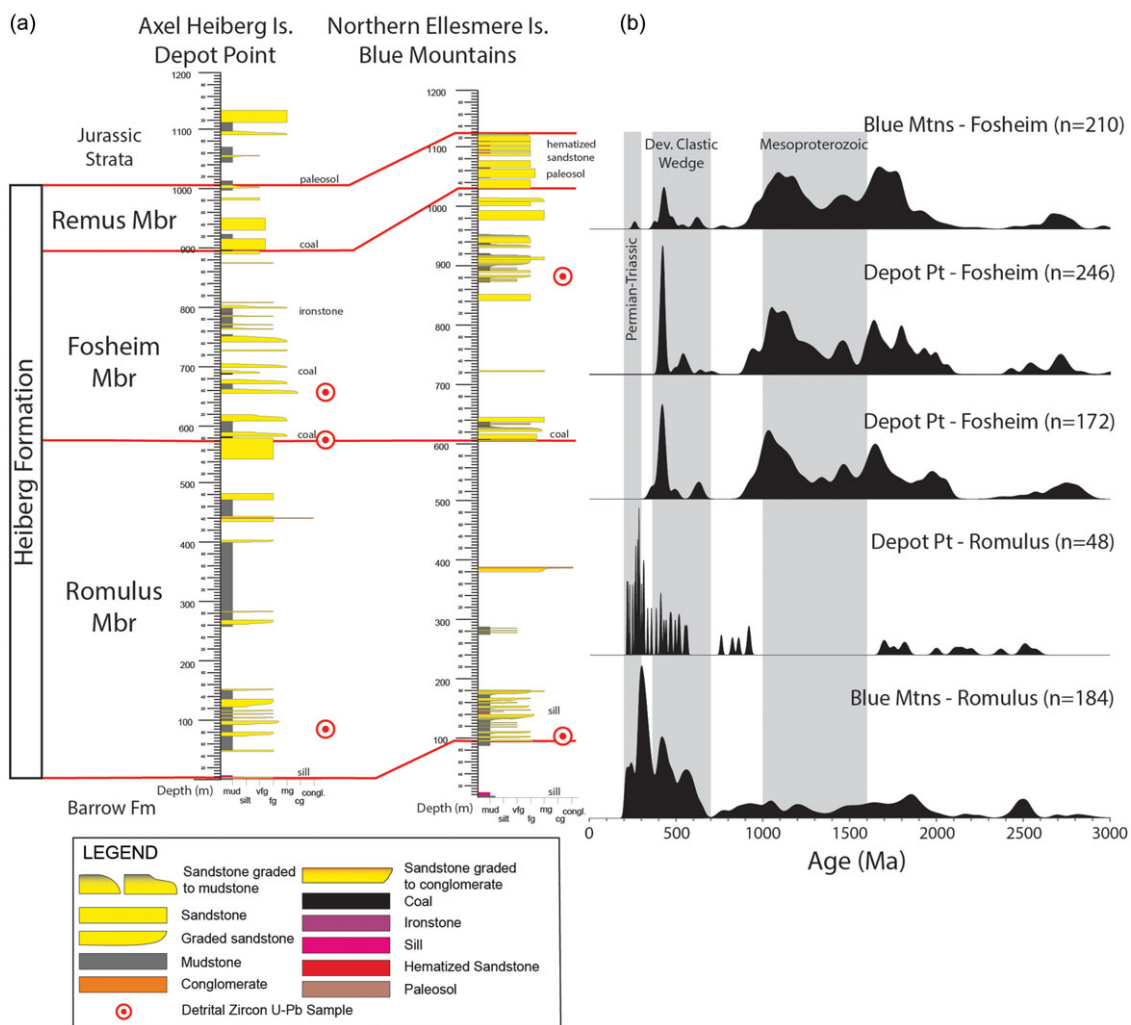


Figure 3. (Colour online) Measured sections (a) with locations of detrital-zircon data (b) presented as normalized probability density functions. Sedimentological data and exact locations of the Blue Mountains and Depot Point sections can be found in Midwinter *et al.* 2021. All U-Pb data from this study, except for the Romulus Member sample from Depot Point (Midwinter *et al.* 2016).

predominantly upper Triassic rocks of Chukotka (Miller *et al.* 2006; Tuchkova *et al.* 2011; Amato *et al.* 2015) and Wrangel Island (Miller *et al.* 2010) resemble the Romulus Member detrital-zircon age spectrum (Figure 4). A detrital-zircon sample from the Mendeleev Rise is similar to upper Triassic samples from Chukotka and Wrangel Island, but with a greater proportion of near-depositional detrital-zircon ages (Tuchkova *et al.* 2020). The Permo-Triassic detrital-zircon age peaks are also found in upper Triassic strata on the Barents Sea side of the Amerasia Basin (Klausen *et al.* 2017), in Svalbard (Bue & Andresen, 2014) and Taimyr (Zhang *et al.* 2016), where they persist through Jurassic strata. The presence of abundant Permo-Triassic detrital zircon in Jurassic strata on Svalbard and near absence in the Sverdrup Basin indicates that the Sverdrup Basin was no longer in sedimentary communication with Svalbard or the Barents shelf in the Early Jurassic (Figure 5). The comparison of detrital-zircon data does not eliminate the transport of sediment from the Sverdrup Basin to the Barents region, but it does preclude the transport of sediment from the Barents region to the Sverdrup Basin. The interpretation of detrital zircon in the Barents shelf region is of provenance from the northern Urals (e.g., Miller *et al.* 2013; Klausen *et al.* 2017; Klausen

et al. 2022), and so if the Sverdrup Basin received such sediment in the Late Triassic, this flux had ceased by the Early Jurassic.

It is possible that part of the provenance change could be due to a cessation of magmatism in the source area, in which case, the 350–215 Ma age fraction would still be present. The virtual absence of the 350–215 Ma fraction indicates that there was an extra-basinal change in sediment routing patterns and even precludes recycling of upper Triassic deposits from the Sverdrup, Barents, Taimyr and the Arctic-Alaska microplate.

Previous work discussed how the Heiberg Formation/Group marks a tectonic transition in the Sverdrup Basin in terms of basin-filling patterns, normal faults and detrital-zircon provenance (Hadlari *et al.* 2016; Midwinter *et al.* 2016). From new U-Pb detrital-zircon dating, we show that the transition occurs at the boundary between the Romulus and Fosheim members. We rely on previous biostratigraphy of the Romulus and Fosheim members to indicate that the timing of this transition is during the latest Triassic (latest Rhaetian). The detrital-zircon age signature of the Fosheim Member is distinct from upper Triassic strata of the Arctic Alaska – Chukotka microplate, and from Jurassic strata of Taimyr and Svalbard. We can therefore state that sediment from

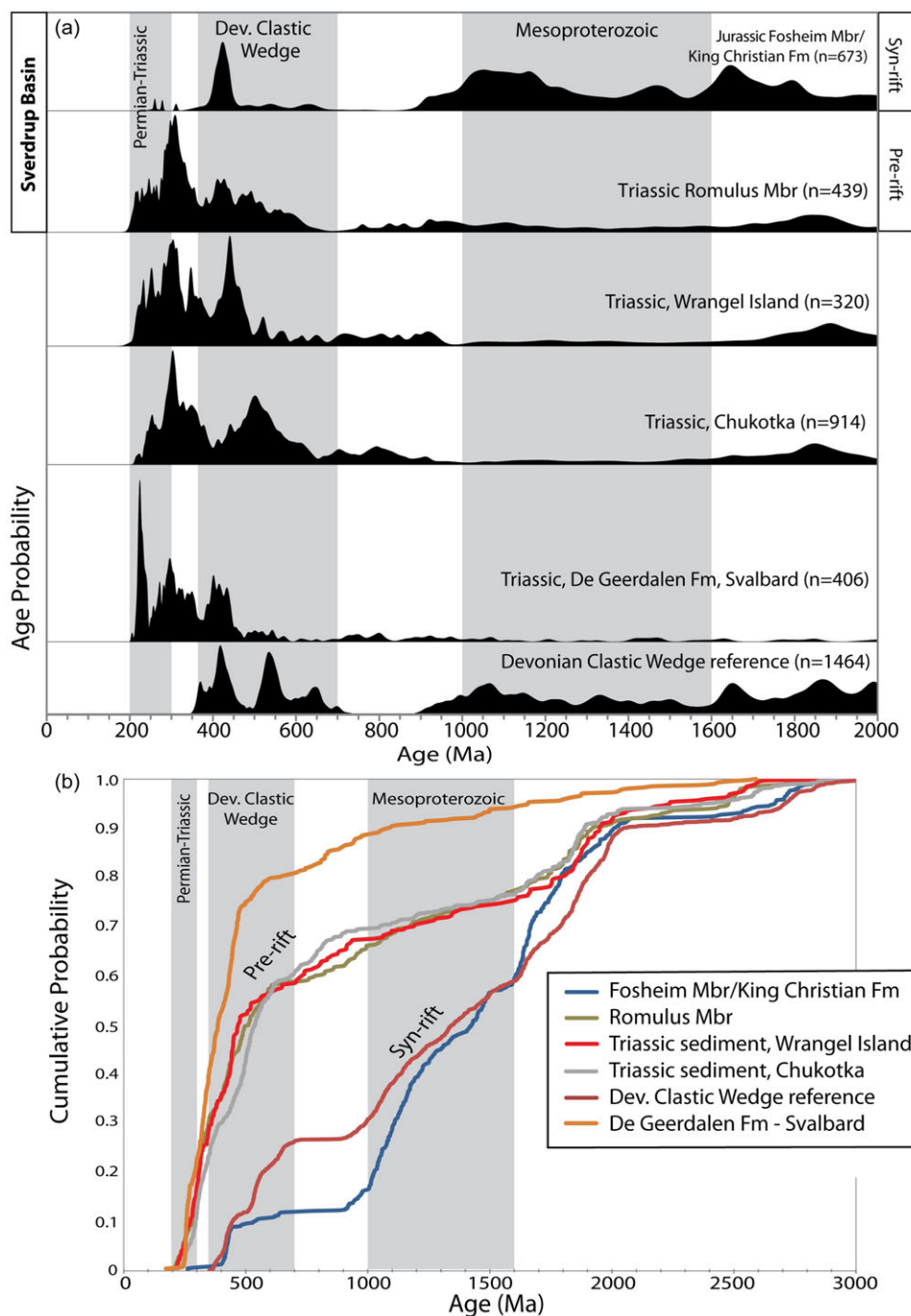


Figure 4. (Colour online) Compiled normalized probability (a) and cumulative probability (b) plots with corresponding number of analyses. Data sources: the Devonian clastic wedge reference spectrum (Anfinson *et al.* 2012a, 2012b); Triassic sediment of Svalbard (Bue & Andresen, 2014); Triassic sediment of Chukotka (Miller *et al.* 2006; Tuchkova *et al.* 2011; Amato *et al.* 2015); Triassic sediment of Wrangel Island (Miller *et al.* 2010); Romulus Mbr. (Midwinter *et al.* 2016; Hadlari *et al.* 2018; this study), Fosheim Mbr./King Christian Fm. (Midwinter *et al.* 2016; this study). ROU: Rift onset unconformity.

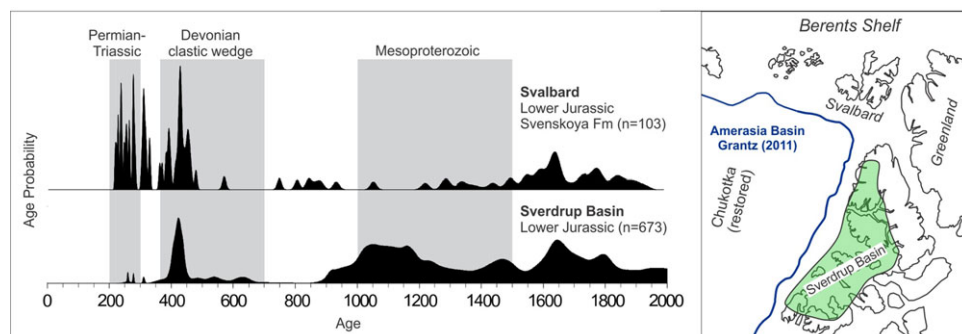


Figure 5. (Colour online) The early Mesozoic position of Svalbard relative to the Sverdrup Basin, based on the palaeogeographic reconstruction of the Amerasia Basin by Grantz (2011). Detrital-zircon U-Pb age spectra from Lower Jurassic strata of the Sverdrup Basin are compared to Svalbard, note the difference in the Permian-Triassic interval (Sverdrup Basin, Midwinter *et al.* 2016, and this study; Bue & Andresen, 2014).

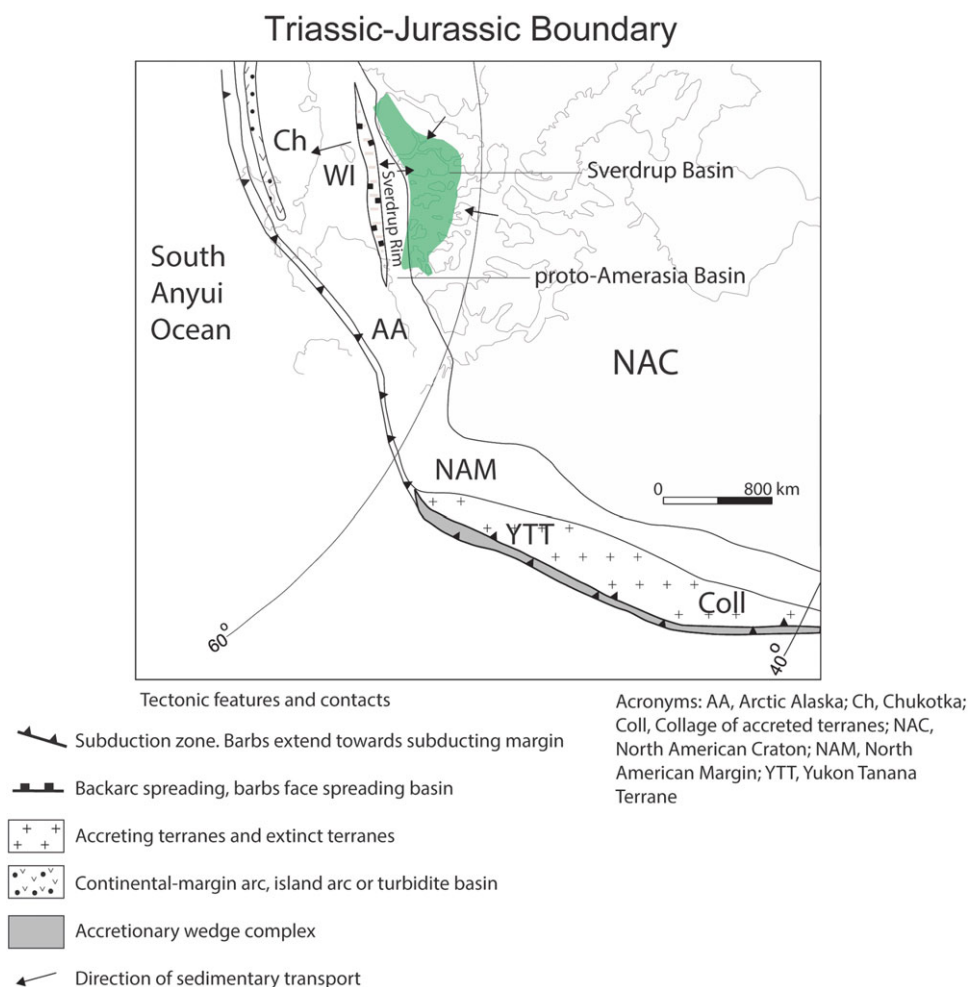


Figure 6. (Colour online) Tectonic environment of northern Laurentia adapted from palaeogeographical maps of Plafker & Berg (1994), Nokleberg *et al.* (2000), and Midwinter *et al.* (2016).

the extra-basinal source of 350–200 Ma detrital zircon had no longer reached the Sverdrup Basin in the lower Jurassic. Based on the similarity to the Devonian clastic wedge, we interpret that the detrital-zircon provenance of the Fosheim Member was sedimentary recycling from erosion of relatively local sedimentary basins, such as the Franklinian Basin, which underlies the Sverdrup Basin (cf. Hadlari *et al.* 2015). Furthermore, we infer that the provenance transition was a response to regional extension (see Hadlari *et al.* 2016), which disrupted sediment transport pathways by the formation of extensional basins that trapped sediment, acting as a sediment sink (cf. Withjack *et al.* 2002; Oliebrook *et al.* 2019). Between the newly-developed proto-Amerasia Basin and the Sverdrup Basin was a palaeo-high, the Sverdrup Rim (Meneley *et al.* 1975), which was a horst that likely prevented sediment from entering the northern part of the Sverdrup Basin and likely acted as a source of sediment for both basins (Figure 6). We interpret that by formation of localized sediment sinks and barriers, the tectonic localization of provenance thereby prevented sediment from the extra-basinal igneous source from reaching the Sverdrup Basin.

6. Conclusion

The upper Triassic to lower Jurassic Heiberg Formation records significant change within the Sverdrup Basin. During deposition of the Romulus Member, the Sverdrup Basin received a large amount of sediment from an extra-basinal igneous source to the northwest

characterized by Carboniferous-Permian-Triassic detrital zircon, and the basin was effectively filled before the end of the late Triassic. Detrital zircon from the Fosheim Member has an age signature that is consistent with an older recycled and more proximal sediment source, similar to the Franklinian Basin, as opposed to a hypothetical Permo-Triassic magmatic arc. We attribute the provenance change from the Romulus to Fosheim members to the onset of extension and rifting that resulted in the initiation of the proto-Amerasia Basin, which acted as a sink and thereby prevented sediment from the northern extra-basinal source area from reaching the Sverdrup Basin.

Supplementary material. The supplementary material for this article can be found at <https://doi.org/10.1017/S0016756824000050>

Acknowledgements. This work was supported by the Geological Survey of Canada and the University of Ottawa. Fieldwork was assisted by the Polar Continental Shelf Program. The manuscript was reviewed by Dr. T.G. Klausen, Dr. J.T. Gooley and five anonymous reviewers.

Competing interests. The authors have no declarations of interest.

References

Amato JM, Toro J, Akinin VV, Hampton BA, Salnikov AS and Tuchkova MI (2015) Tectonic evolution of the Mesozoic South Anyui suture zone, eastern Russia: a critical component of paleogeographic reconstructions of the Arctic region. *Geosphere* 11(5), 1530–1564.

- Anfinson OA, Embry AF and Stockli DF** (2016) Geochronologic constraints on the Permian–Triassic northern source region of the Sverdrup Basin, Canadian Arctic Islands. *Tectonophysics* **691**, 206–219.
- Anfinson OA, Leier AL, Embry AF and Dewing K** (2012a) Detrital zircon geochronology and provenance of the Neoproterozoic to Late Devonian Franklinian basin, Canadian Arctic Islands. *Geological Society of America Bulletin* **124**(3–4), 415–430.
- Anfinson OA, Leier AL, Gaschnig R, Embry AF and Dewing K** (2012b) U–Pb and Hf isotopic data from Franklinian Basin strata: insights into the nature of Crockerland and the timing of accretion, Canadian Arctic Islands. *Canadian Journal of Earth Sciences* **49**(11), 1316–1328.
- Alonso-Torres D, Beauchamp B, Guest B, Hadlari T and Matthews WA** (2018) Late Paleozoic to Triassic arc magmatism north of the Sverdrup Basin in the Canadian Arctic: Evidence from detrital zircon U–Pb geochronology. *Lithosphere* **10**(3), 426–445.
- Balkwill HR** (1978) Evolution of Sverdrup Basin. *American Association of Petroleum Geologists Bulletin* **62**, 1004–1028.
- Bue EP and Andresen A** (2014) Constraining depositional models in the Barents Sea region using detrital zircon U–Pb data from Mesozoic sediments in Svalbard. *Geological Society, London, Special Publications* **386**, 261–279.
- Cawood PA, Hawkesworth C and Dhuime B** (2012) Detrital zircon record and tectonic setting. *Geology* **40**, 875–878.
- Coutts DS, Matthews WA and Hubbard SM** (2019) Assessment of widely used methods to derive depositional ages from detrital zircon populations. *Geoscience Frontiers* **10**, 1421–1435.
- Dickinson WR and Gehrels GE** (2009) Use of U–Pb ages of detrital zircons to infer maximum depositional ages of strata: a test against a Colorado Plateau Mesozoic database. *Earth and Planetary Science Letters* **288**(1–2), 115–125.
- Drachev SS** (2011) Tectonic setting, structure and petroleum geology of the Siberian Arctic offshore sedimentary basins. *Geological Society of London Memoirs* **35**, 369–394.
- Embry AF** (1983a) Stratigraphic subdivision of the Heiberg Formation, eastern and central Sverdrup Basin, Arctic Islands. *Geological Survey of Canada Current Research* **83-1B**, 205–213.
- Embry AF** (1983b) The Heiberg Group, western Sverdrup Basin, Arctic Islands. *Geological Survey of Canada Current Research* **83-1B**, 381–389.
- Embry AF** (1991) Mesozoic history of the Arctic Islands. In *Inuitian Orogen and Arctic Platform: Canada and Greenland Volume 3* (ed HP Trettin), pp. 369–433. Geological Survey of Canada, Geology of Canada (DNAG).
- Embry AF** (2009) Crockerland—the source area for the Triassic to Middle Jurassic Strata of Northern Axel Heiberg Island, Canadian Arctic Islands. *Bulletin of Canadian Petroleum Geology* **57**(2), 129–140.
- Embry AF and Beauchamp B** (2008) Sverdrup Basin. In *The Sedimentary Basins of the United States and Canada* (ed AD Miall), pp. 451–471. Amsterdam, The Netherlands: Elsevier.
- Embry AF and Johannessen EP** (1993) T–R sequence stratigraphy, facies analysis and reservoir distribution in the uppermost Triassic–Lower Jurassic succession, western Sverdrup Basin, Arctic Canada. In *Arctic Geology and Petroleum Potential* (eds TO Vorren), pp. 121–146. Norwegian Petroleum Society, Special Publication no. 2.
- Embry AF and Suneby LB** (1994) The Triassic–Jurassic boundary in the Sverdrup Basin, Arctic Canada. *Canadian Society of Petroleum Geologists, Memoir* **17**, 858–869.
- Gilmullina A, Klausen TG, Dore AG, Sirevaag H, Suslova A and Eide CH** (2022) Arctic sediment routing during the Triassic: sinking the Arctic Atlantis. *Journal of the Geological Society* **180**(1): jgs2022-018.
- Gottlieb ES, Meisling KE, Miller EL and Charles G** (2014) Closing the Canada Basin: Detrital zircon geochronology relationships between the North Slope of Arctic Alaska and the Franklinian mobile belt of Arctic Canada. *Geosphere* **10**(6), 1366–1384.
- Grantz A, Eittreim S and Dinter DA** (1979) Geology and tectonic development of the continental margin north of Alaska. *Tectonophysics* **59**(1), 263–291.
- Grantz A, Hart PE and Childers VA** (2011) Geology and tectonic development of the Amerasia and Canada Basins, Arctic Ocean. *Geological Society of London Memoirs* **35**, 771–799.
- Hadlari T, Dewing K, Matthews WA, Alonso-Torres D and Midwinter D** (2018) Early Triassic development of a foreland basin in the Canadian high Arctic: Implications for a Pangean Rim of Fire. *Tectonophysics* **736**, 75–84.
- Hadlari T, Midwinter D, Galloway JM, Dewing K and Durbano AM** (2016) Mesozoic rift to post-rift tectonostratigraphy of the Sverdrup Basin, Canadian Arctic. *Marine and Petroleum Geology* **76**, 148–158.
- Hadlari T, Midwinter D, Poulton TP and Matthews WA** (2017) A Pangean rim of fire: Reviewing the Triassic of western Laurentia. *Lithosphere* **9**(4), 579–582.
- Hadlari T, Swindles GT, Galloway JM, Bell KM, Sulphur KC, Heaman LM, Beranek LP and Fallas KM** (2015) 1.8 billion years of sedimentary recycling calibrates a refractory part of Earth’s sedimentary cycle. *PLoS ONE* **10**, e0144727.
- Houseknecht DW and Bird KJ** (2011) Geology and petroleum potential of the rifted margins of the Canada Basin. *Geological Society of London Memoirs* **35**, 509–526.
- Klausen TG, Muller R, Slama J and Helland-Hansen W** (2017) Evidence for Late Triassic provenance areas and Early Jurassic sediment supply turnover in the Berents Sea Basin of northern Pangea. *Lithosphere* **9**, 14–28.
- Klausen TG, Rismyhr B, Muller R and Olausen S** (2022) Changing provenance and stratigraphic signatures across the Triassic–Jurassic boundary in eastern Spitsbergen and the subsurface Barents Sea. *Norwegian Journal of Geology* **102**, 202205
- Lopez-Mir B, Schneider S and Hülse P** (2018) Fault activity and diapirism in the Mississippian to Late Cretaceous Sverdrup Basin: New insights into the tectonic evolution of the Canadian Arctic. *Journal of Geodynamics* **118**, 55–65.
- Matthews WA and Guest B** (2017) A practical approach for collecting large-n detrital zircon U–Pb data sets by quadrupole LA–ICP–MS. *Geostandards and Geoanalytical Research* **41**(2), 161–180.
- Meneley RA, Henao D and Merritt RK** (1975) The northwest margin of the Sverdrup Basin. In *Canada’s Continental Margins and Offshore Petroleum Exploration* (eds CJ Yorath), pp. 557–587. Canadian Society of Petroleum Geologists, Special Publication no. 4.
- Midwinter D, Hadlari T, Davis WJ, Dewing K and Arnott RWC** (2016) Dual provenance signatures of the Triassic northern Laurentian margin from detrital zircon U–Pb and Hf isotope analysis of Triassic–Jurassic strata in the Sverdrup Basin. *Lithosphere* **8**(6), 668–683.
- Midwinter D, Hadlari T and Dewing K** (2022) Upper Triassic to Lower Jurassic stratigraphy along the northeastern margin of the Sverdrup Basin, Axel Heiberg and Ellesmere islands, Nunavut: new data from measured sections. *Geological Survey of Canada, Open File* **8855**, 17.
- Miller EL, Gehrels GE, Pease V and Sokolov S** (2010) Stratigraphy and U–Pb detrital zircon geochronology of Wrangel Island, Russia: Implications for Arctic paleogeography. *American Association of Petroleum Geologists Bulletin* **94**(5), 665–692.
- Miller EL, Soloviev AV, Prokopiev AV, Toro J, Harris D, Kuzmichev AB and Gehrels GE** (2013) Triassic river systems and the paleo-Pacific margin of northwestern Pangea. *Gondwana Research* **23**, 1631–1645.
- Miller EL, Toro J, Gehrels G, Amato JM, Prokopiev A, Tuckkova MI, Akinin VV, Dumitru TA, Moore TE and Cecile MP** (2006) New insights into Arctic paleogeography and tectonics from U–Pb detrital zircon geochronology. *Tectonics* **25**(3), 1–19.
- Nokleberg WJ, Parfenov LM, Monger JW, Norton IO, Chanduk AI, Stone DB, Scotese CR, Scholl DW and Fujita K** (2000) *Phanerozoic tectonic evolution of the Circum-North Pacific*. United States Geological Survey, Professional Paper no. 1626, 122 pp.
- Okulitch AV**, Compiler (1991) *Geology of the Canadian Archipelago, Northwest Territories and North Greenland*. Geological Survey of Canada, Map 1715A, scale 1:2,000,000.
- Oliefbrook HKH, Barham M, Fitzsimons ICW, Timms NE, Jiang Q, Evans NJ and McDonald BJ** (2019) Tectonic controls on sediment provenance evolution in rift basins: Detrital zircon U–Pb and Hf isotope analysis from the Perth Basin, Western Australia. *Gondwana Research* **66**, 126–142.
- Omnia JE, Pease V and Scott RA** (2011) U–Pb SIMS zircon geochronology of Triassic and Jurassic sandstones on northwestern Axel Heiberg Island, northern Sverdrup Basin, Arctic Canada. In *Arctic Petroleum Geology* (eds AM Spencer, D Gautier, A Stoupakova, A Embry & K Sørensen), v. 35, pp. 559–566. Geological Society of London Memoir.
- Piejohn K and Von Gosen W** (2018) Structural transect through Ellesmere Island (Canadian Arctic): superimposed Palaeozoic Ellesmerian and

- Cenozoic Eureka deformation. *Geological Society, London, Special Publications* **460**, 33–56.
- Plafker G and Berg HC** (1994) Overview of the geology and tectonic evolution of Alaska. In *The Geology of Alaska* (eds G Plafker & HC Berg), pp. 989–1021. Geological Society of America, Geology of North America, v. G-1.
- Pointon MA, Smyth H., Omma JE, Morton AC, Schneider S, Hulse P, Ripington SJ, Lopez-Mir B, Crowley QG, Millar I, Whitehouse MJ, Frei D, Scott RA and Flowerdew MJ** (2023) A multi-proxy provenance study of Late Carboniferous to Middle Jurassic sandstones in the Eastern Sverdrup Basin and its bearing on Arctic Paleogeographic reconstructions. *Geosciences* **13**(10), 41.
- Souther JG** (1963) Geological traverse across Axel Heiberg Island from Buchanan Lake to Strand Fiord, in Geology of the north central part of the Arctic Archipelago, Northwest Territories (Operation Franklin). *Geological Survey of Canada Memoir* **320**, 426–448.
- Suneby LB and Hills LV** (1988) Palynological zonation of the Heiberg Formation (Triassic-Jurassic) eastern Sverdrup Basin, Arctic Canada. *Bulletin of Canadian Petroleum Geology* **36**(4), 347–361
- Tuchkova MI, Sokolov SD, Khudoley AK, Verzhbitsky VE, Hayasaka Y & Moiseev AV** (2011) Permian and Triassic deposits of Siberian and Chukotka passive margins: sedimentation setting and provenances. Proceedings of the International Conference on Arctic Margins VI, Fairbanks, Alaska, 61–96.
- Tuchkova MI, Shokalsky SP, Petrov OV, Sokolov SD, Sergeev SA and Moiseev AV** (2020) Triassic deposits of Chukotka, Wrangel Island and Mendeleev Rise, Arctic Sea: sedimentology and geodynamic implications. *GFF (Journal of the Geological Society of Sweden)* **142**(2), 158–168.
- Withjack MO, Schlische R and Olsen PE** (2002) Rift-basin structure and its influence on sedimentary systems, in sedimentation in continental rifts. *SEPM Special Publication* **73**, 57–81.
- Zhang X, Pease V, Skogseid J and Wohlgemuth-Ueberwasser CW** (2016) Reconstructions of tectonic events on the northern Eurasian margin of the Arctic, from U-Pb detrital zircon provenance investigations of late Paleozoic to Mesozoic sandstones in southern Taimyr Peninsula. *GSA Bulletin* **128**, 29–46.